The Topology of Networks and Cortical Synchrony

Stephanie M. Nelli Aaron L. Sampson Patrick S. Strassmann

BGGN/BENG 260 Neurodynamics
University of California, San Diego
La Jolla, CA 92093

Abstract

In cortex, there are several electrically coupled inhibitory interneuronal networks which are thought to be critical to temporal coordination of cortical and hippocampal oscillations seen in EEG. This is because gap-junction mediated networks have many properties, such as speed and bidirectionality, desirable for neural synchronization. Gap junctions exclusively connect GABAergic neurons of the same type, implying distinct functional roles for each type of inhibitory network. Using BRIAN, we built a model simulating Layer IV excitatory neurons, which receive thalamic input and synapse onto gap-junction coupled interlaminar inhibitory neurons, which in turn inhibit Layer VI excitatory neurons. The electrical coupling of the inhibitory layer drives synchronization of neuronal firing in Layer VI which is dependent on the topology the electrically connected inhibitory network. We investigated how lattice (nearest neighbor), random, and small world topologies effect synchronization. Small world networks occur when a percent of connections in a lattice network are rewired randomly, resulting in the path length L between any two neurons scaling with the logarithm of N. Small world networks are less likely to exist in systems where links arise mainly from spatial or temporal proximity. We found that small-world network topology for the gap-junction connected inhibitory network results in the highest correlation between spiking of neurons in the inhibited layer.

1 Introduction

The neocortex is the outermost layer of the human brain, containing 6 morphologically and functionally distinct layers, with layer IV receiving thalamic input and layer VI sending afferents to the thalamus. At rest, or without stimulation, excitatory networks exhibit independent and sparse firing. However, in recent years understanding the neuronal underpinnings of cortical rhythms has attracted significant attention. In the waking brain, small-amplitude EEG signals are largely asynchronous, with weak, intermittent synchrony exhibiting temporal and spatial selectivity ([1]-[2]). Single neurons seem to exhibit Poisson processes ([1]-[2]). Excitatory synchrony is a result of action potentials highly correlated in time, which is key for a variety of important neural mechanisms such as spike timing dependent plasticity, sensory coding, and gain modulation ([3]). Interplay between excitatory and inhibitory neocortical neurons is essential for synchronous activity ([3]-[4]). Synaptic inhibition likely sculpts the temporal activity patterns of cortical activity. In 1999, Gibson et al. found extensive gap junction coupling between inhibitory interneurons of the same type in neocortex. This suggests that these inhibitory networks have distinct, perhaps

input specific, roles in temporally sculpting excitation through quick and bidirectional gap junction coupling.

While these electrically coupled inhibitory networks are likely important for fast cortical oscillations, the general connectivity of these networks is unknown. Cortical oscillations necessitate a threshold level of synchrony; in randomly connected Hodgkin-Huxley models almost 50 synapses per neurons are necessary ([1]-[3]), while in our model this number is greatly reduced, presumably due to gap junction coupling. However, cortical networks are likely not randomly connected, and networks that exhibit dense local clustering and sparse long-range connections are more plausible. Thus, our goal in the current analysis was to determine how the topology of an electrically coupled inhibitory network in neocortex receiving input from cortical layer IV could contribute to synchronization of spiking in layer VI.

2 Hodgkin-Huxley model

All simulations were done in BRIAN, a python neural network simulator. We simulated 2400 excitatory and 800 inhibitory neurons with membrane potential described by the differential equation: $\frac{dv}{dt} = \frac{I_m}{C_m} + \frac{\sigma * x_i}{tau}$, where x_i is a keyword in BRIAN for Gaussian noise experiencing a standard deviation σ = 0.4 and τ = 15 seconds in our simulation. $I_m = I_e + I_{Na} + I_K + I_{leak} + I_{gap}$, where $I_{gap} = w * (v_{pre} - v_{post})$ in inhibitory neurons, and =0 otherwise. We also modeled the opening and closing of ionic channels and their respective differential equations (see supplementary materials).

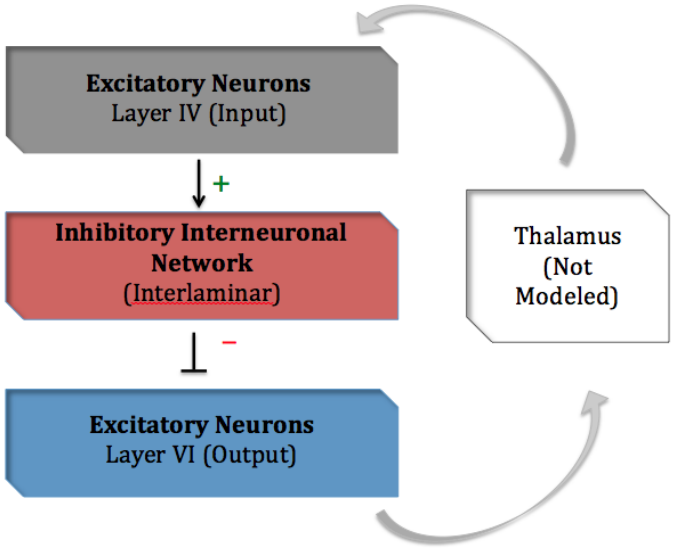

Figure 1: Cortical model

3 Cortical model

Our model is intended to simulate connectivity between three cortical layers: layer IV, layer VI, and an inhibitory interneuronal layer that connects the two. Layer IV and layer VI consisted of 1200 neurons each, whereas the inhibitory layer consisted of 800 neurons. Layer IV excitatory neurons received 2 µA of excitatory input to model thalamocortical neuronal input. Layer IV was connected to the inhibitory network with 40% sparseness. These inhibitory neurons were then connected to the layer VI with a 10% sparseness. Our conceptual model is outlined in Figure 1.

4 Inhibitory connectivity

Three topologies were investigated among the 800 neuron inhibitory network. First, we investigated a regular lattice network of local neighbor-to-neighbor connections (Fig 2A). In this network, each of the 800 neurons was connected to nine neighboring neurons. Second, we constructed a network of random connections (Fig 2B) with a sparseness of 2%. Lastly, a small-world network was created following the Newman-Watts methodology ([6]), (Fig 2C). This network was derived from the network of regularly connected neighbors, and additional nonlocal connections were added with a specified probability of 0.5 for each neuron. The three networks were constrained to have a total number of connections varying by no more than 6%. All networks were defined with symmetric connection matrices to reflect the bidirectionality of electrical synapses. It was found that the weight of inhibitory connections had an effect on the coefficient of variation, the ratio of the standard deviation over the mean of spike timing for a particular neuron, for layer VI neurons. Example neighbor-to-neighbor, random, and small world networks (respectively) are shown to the right in Figure 2, and network characteristics are in the supplementary information.

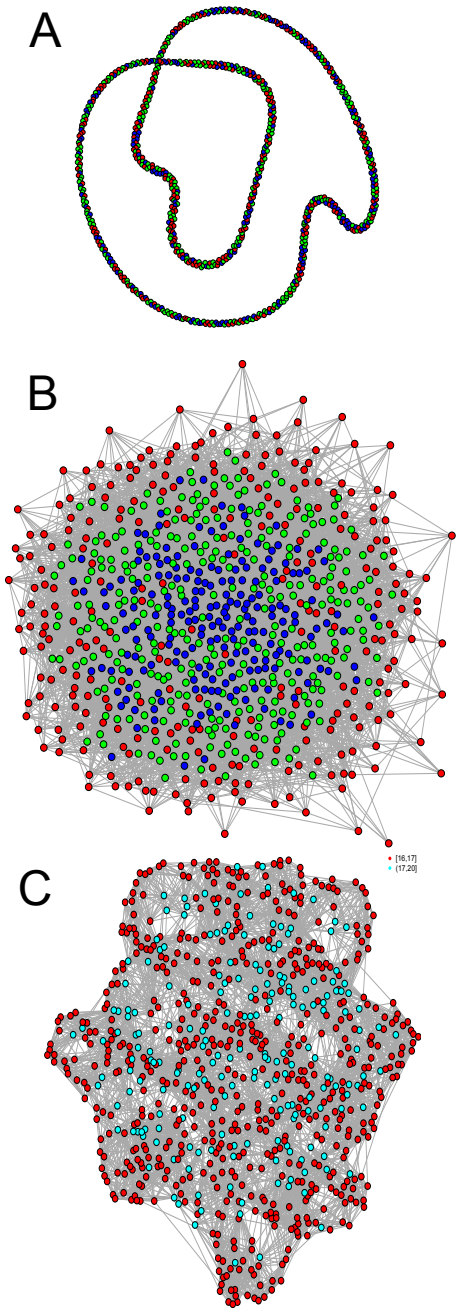

Figure 2: Inhibitory network topology

5 Results

Figures 3, 4, and 5 show BRIAN plots of our cortical model with inhibitory networks of 'regular', 'random', and 'small world' topologies respectively. For each figure, the top three subplots are raster plots showing the temporal location of individual action potentials for every neuron in the designated layer. A single point on the graph represents an action potential, with the y-axis designating the individual neuron (labeled 1-1200, or 1-800 for the inhibitory layer), and the x-axis designating the time at which the action potential occurs. The bottom subplots of each figure show voltage traces of a single, representative neuron from each layer.

For each topology, spontaneous and random firing can be seen in Layer VI in the absence of inhibitory connections (Figures 3A, 4A, 5A). As mentioned in the description of our model, this spontaneous firing was achieved using a Gaussian noise current. In these figures, one can also observe a perceptibly denser firing pattern in layer IV that, in addition to the same Gaussian noise current, also includes an external simulation of 2 μA to simulate thalamic input. As expected, action potentials are tightly temporally coordinated in the inhibitory layers, a result of the fast, bidirectional electrical coupling via gap junctions.

When the inhibitory layer is connected to Layer VI, tight, oscillatory synchronization is clearly observed in temporal coordination with the firing pattern of the inhibitory layers (Figures 3B, 4B, 5B). Visually, the extent of Layer VI synchronization is not perceptibly different between the tested inhibitory network topologies. However, when quantitatively investigated we found differences between the degree of synchronization across the inhibitory network topological types.

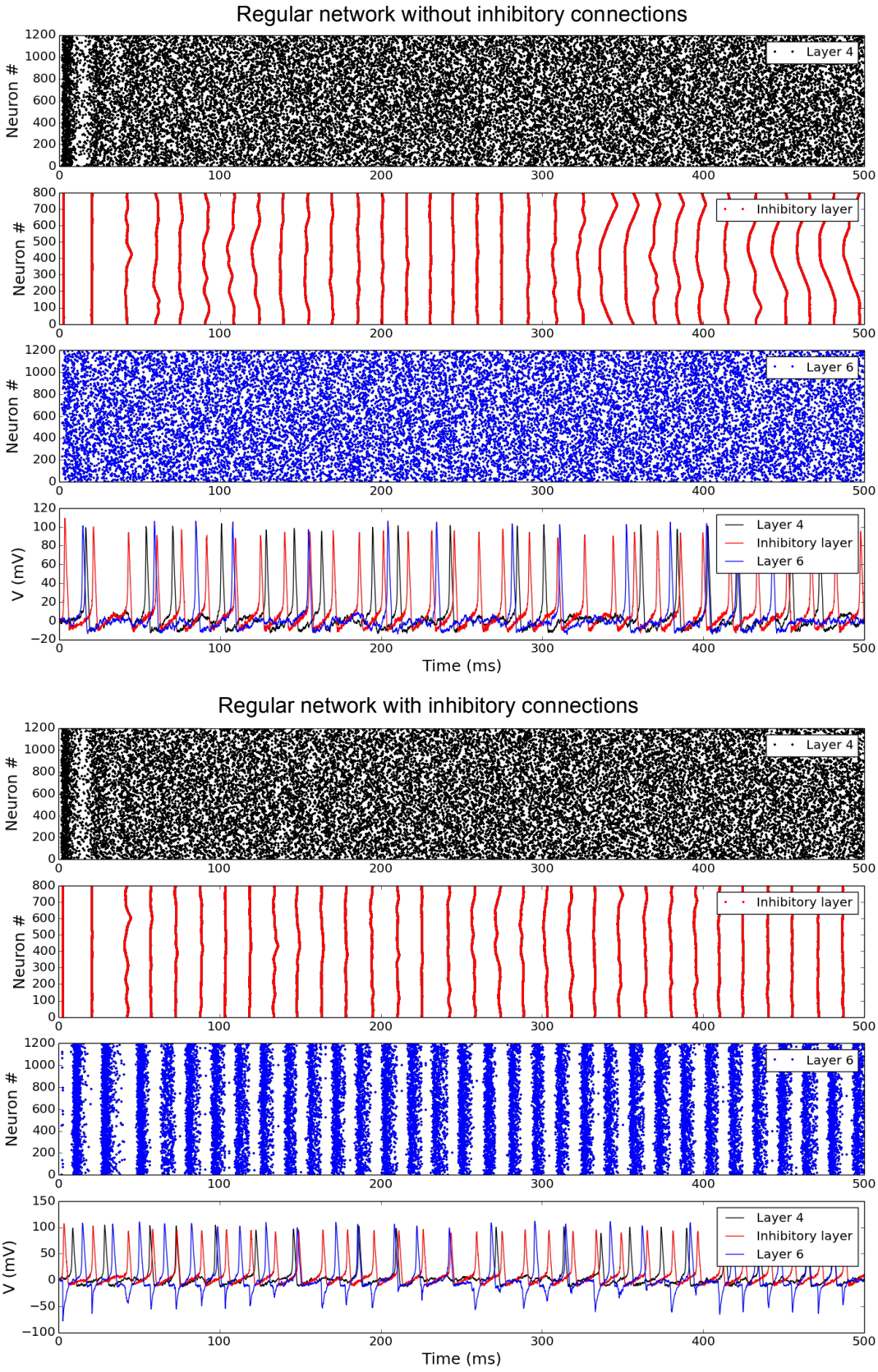

131 Figure 3: Regular topology, with and without inhibitory connections to Layer VI

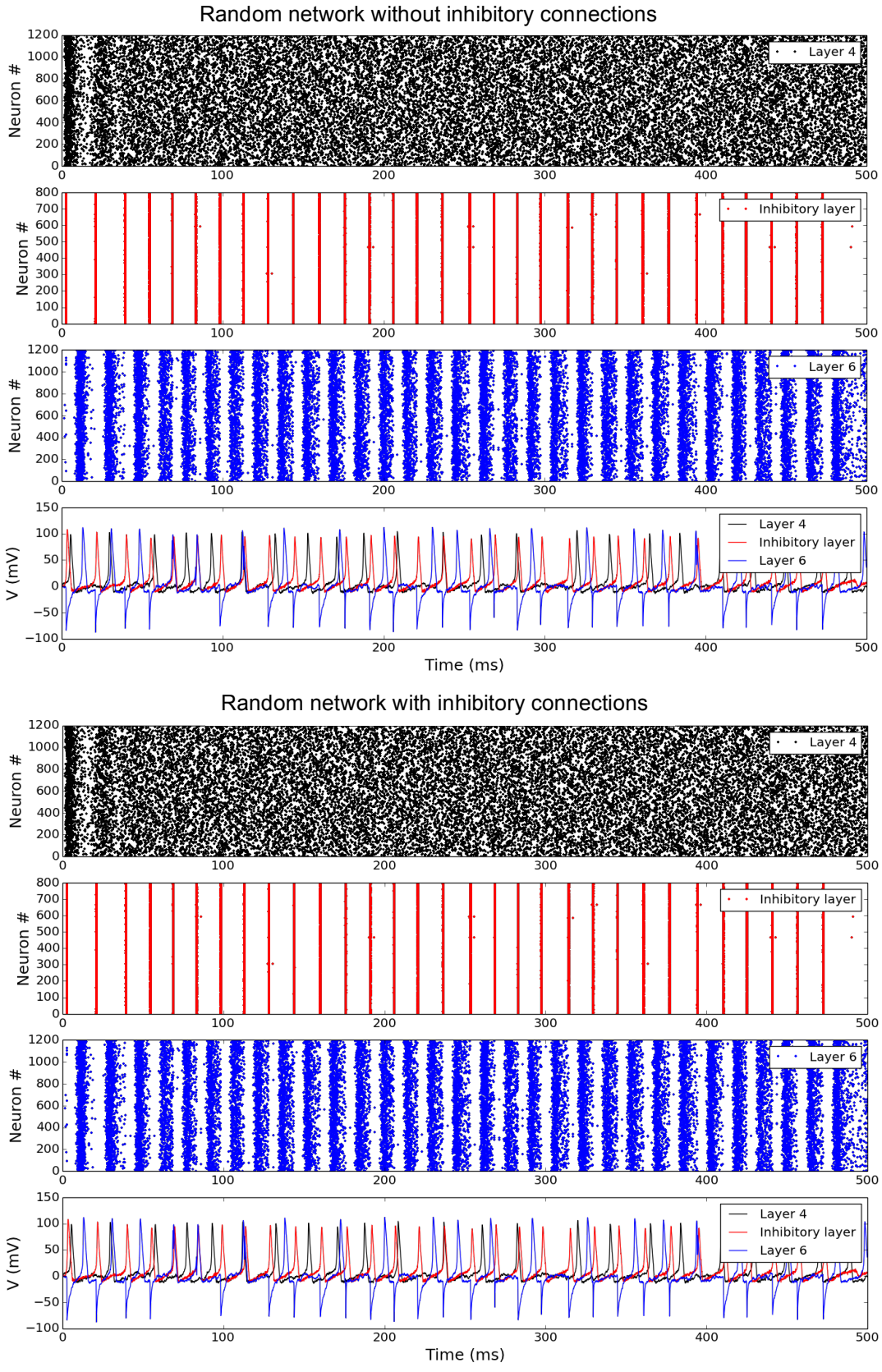

132 Figure 4: Random topology, with and without inhibitory connections to Layer VI

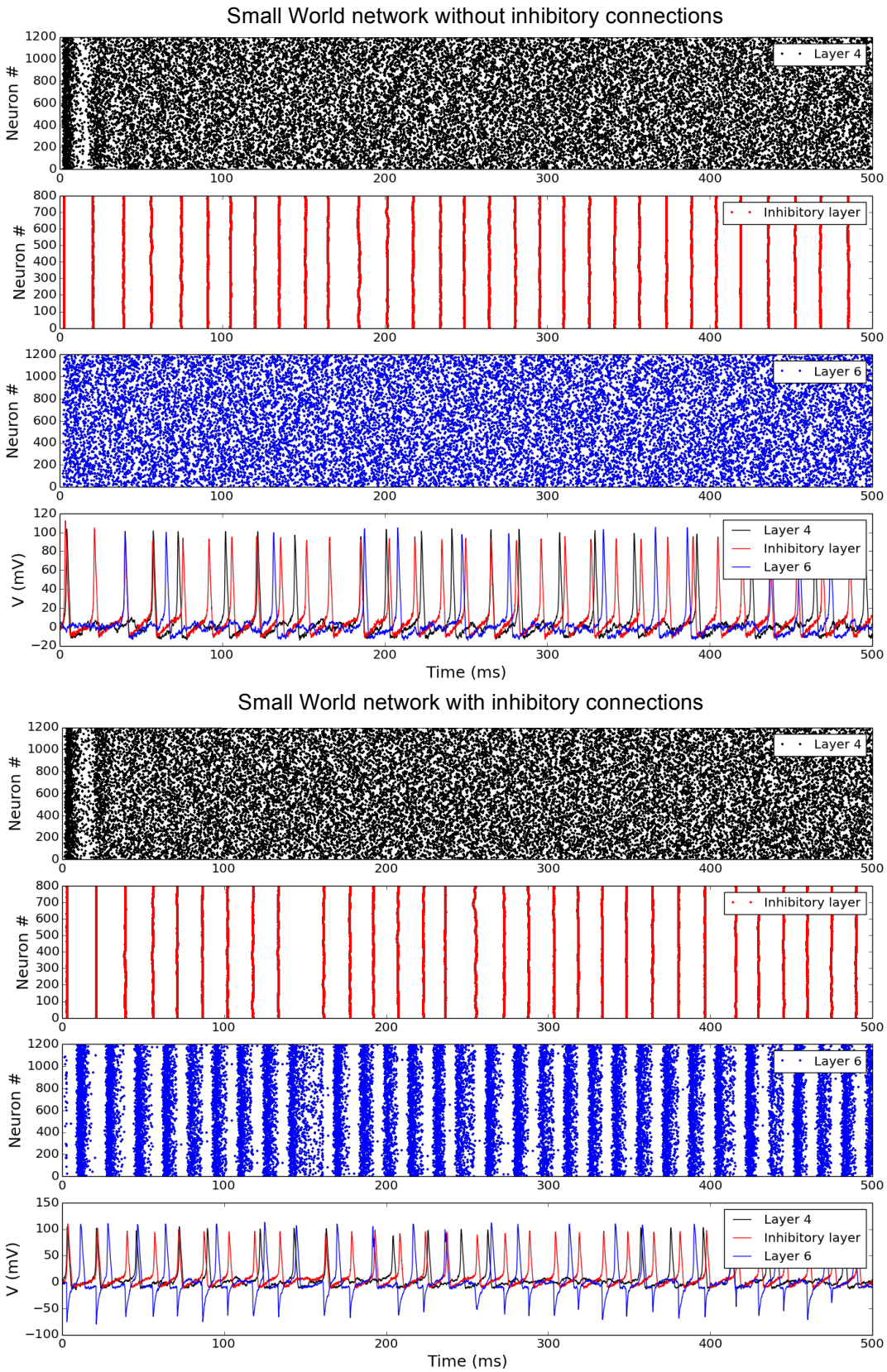

133 Figure 5: Small world topology, with and without inhibitory connections to Layer VI

The synchrony of firing in the inhibited layer VI excited neurons was evaluated using cross-correlation tools in BRIAN. Correlograms, shown in Figure 6, were computed by comparing a single test neuron to all other neurons in the layer. The spikes were compared in 1 ms bins and compared within 100 ms before and after the initial spike. Figure X shows the same test neuron from layer VI and it's cross-correlation with all other layer VI excitatory neurons, plotted separately for inhibition by regularly, randomly, and small-world connected inhibitory networks. While all inhibitory network topologies effectively synchronize layer VI, and clearly show the highest correlation value for zero time shift, the values of the correlation differ, the highest values of correlation are displayed by the small-world network (note the color scales in Figure 6).

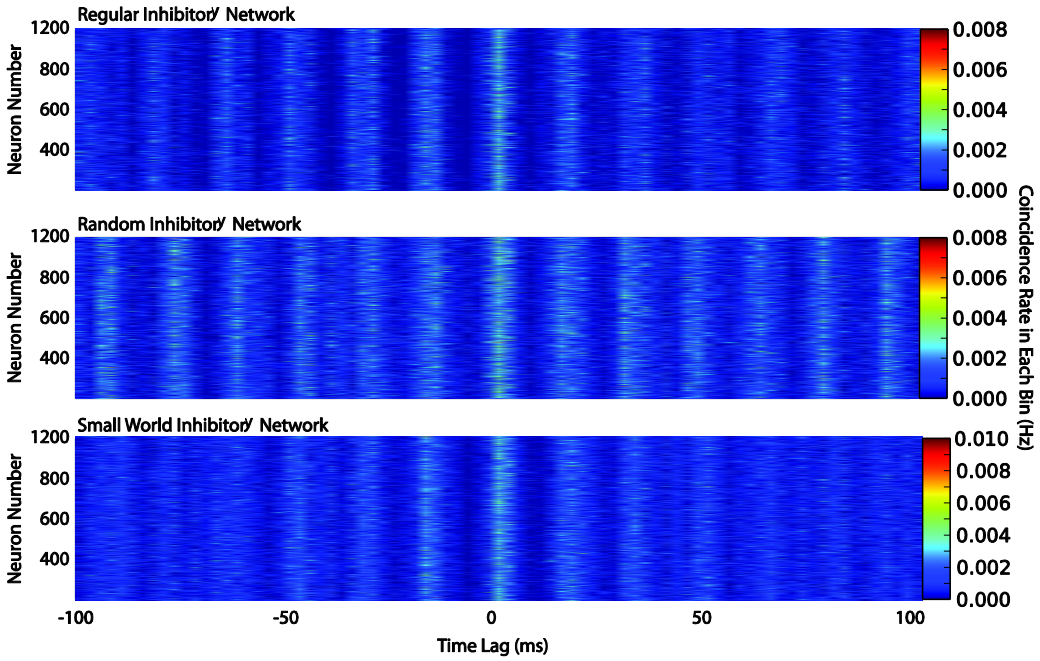

Figure 6: Layer VI correlograms for regular, random, and small world inhibitory networks

Since the small world network exhibited the greatest degree of synchrony, we then investigated how the degree of gap junction coupling affected synchrony using the coefficient of variation (standard deviation/mean), a measure of spike-noise at the level of the individual neuron. We simulated the network 5 times for each value of gap junction conductance investigated between 0-0.85 millisiemens. These values are shown in Figure 7. There is a general trend toward a higher coefficient of variation for higher values of gap junction conductance.

6 Discussion and future directions

These results demonstrate how the synchronous firing of large populations of neurons can be driven by an inhibitory interneuronal network coupled via gap junctions. In particular, we have demonstrated how the network topologies of an electrically connected inhibitory layer impacts the degree of synchronization in the inhibited layer, and demonstrated the value of the low path length and high clustering of the small world network.

We would like to further investigate complex topologies and their effects on synchronization, such as scale free network models. Importantly, we would like to achieve biophysical specificity in neuronal subtypes across the layers, which were not implemented in this model. We could then investigate how different inhibitory cell types, such as the well-known fast spiking and low threshold spiking interneuron types, may interact with coupling topologies. Furthermore, we are working on an expanded cortical model including the inter-layer processing that occurs in layer II/III before thalamic input reaches layer VI.

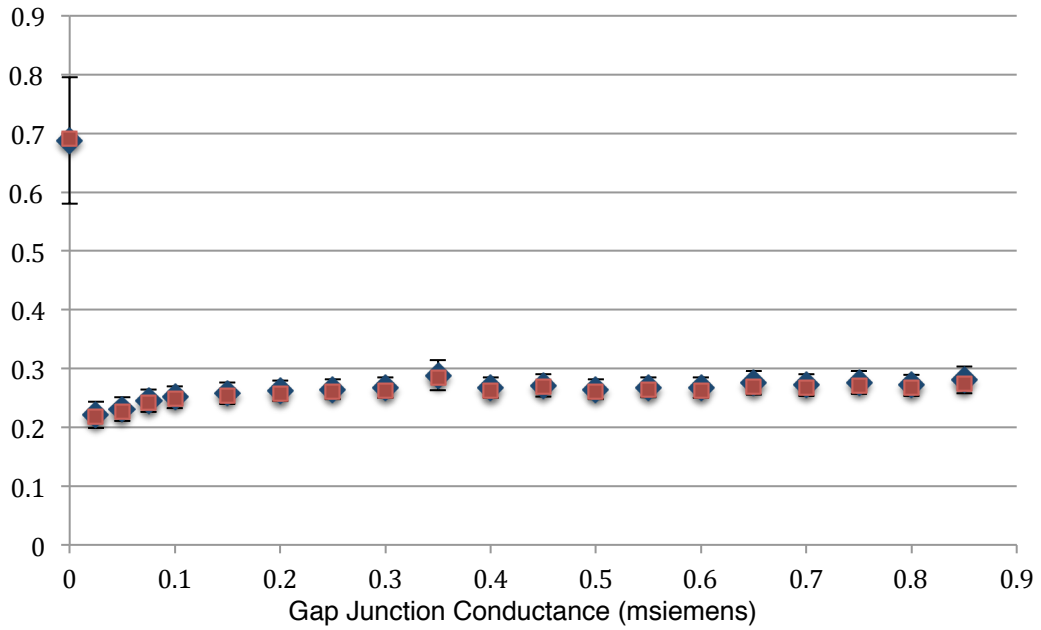

Figure 7: Average layer VI spike variation depends on strength of gap junction coupling

7 Supplementary Materials

Gating equations:

Opening:

$$\propto_h = 0.7 * e^{-0.5}$$

$$\propto_m = 0.1 * \frac{25 - v_m}{e^{2.5-0.1*v_m} - 1}$$

$$\propto_n = 0.01 * \frac{10 - v_m}{e^{1-0.1*v_m} - 1}$$

Closing:

$$\beta_h = \frac{1}{1 + e^{3-0.1*v_m}}$$

$$\beta_m = 4 * e^{-0.0556*v_m}$$

$$\beta_n = 0.125 * e^{-0.0125*v_m}$$

Dynamics:

$$\frac{dh}{dt} = \propto_h * (1 - h) - \beta_h * h$$

$$\frac{dm}{dt} = \propto_m * (1 - m) - \beta_m * m$$

$$\frac{dn}{dt} = \propto_n * (1 - n) - \beta_n * n$$

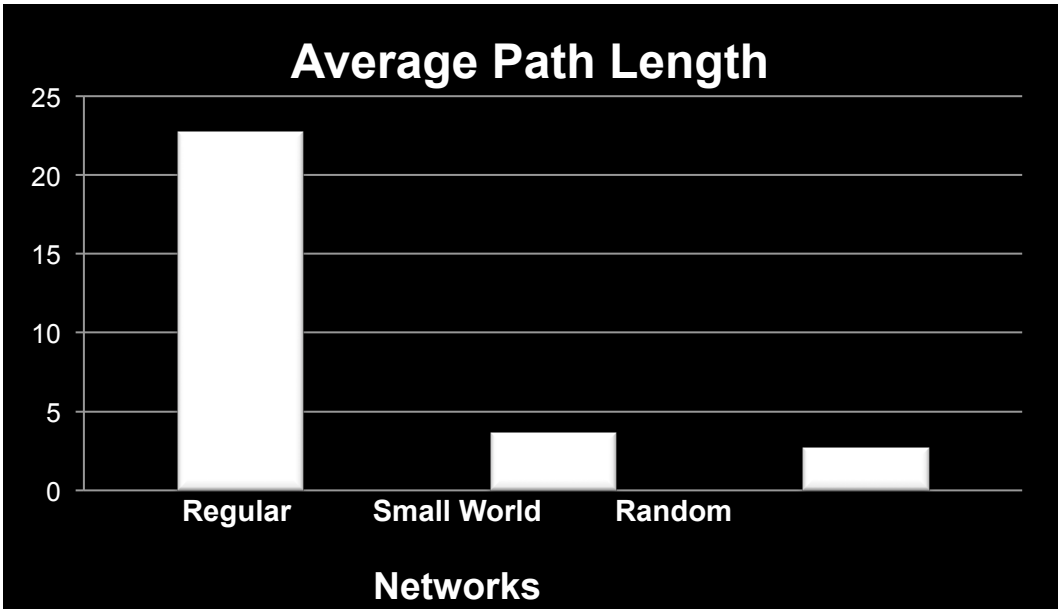

Figure 8: The average length of any two neurons in the simulated networks

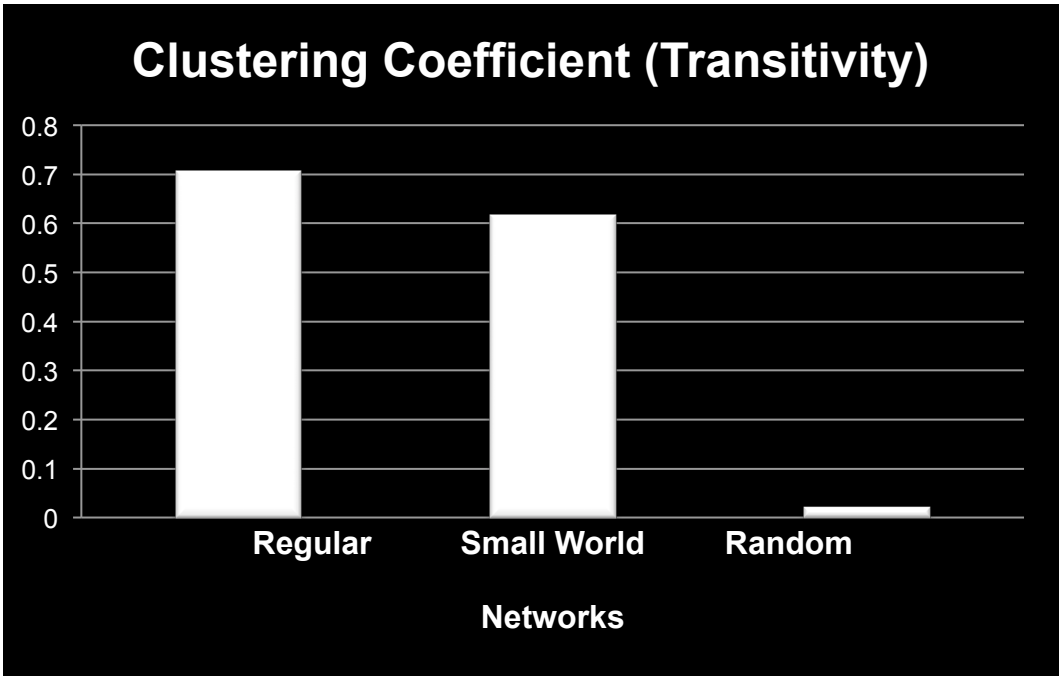

Figure 9: The probability that if neuron X is connected to Y and Y is connected to Z such that X is also connected to Z

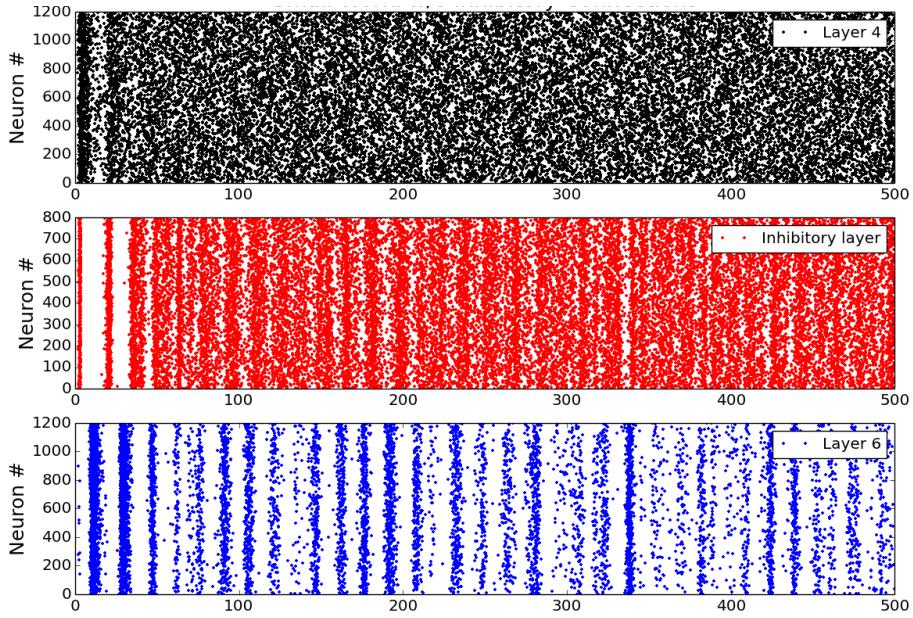

Figure 10: Small World Network with (nearly) 0 mS gap junction conductance

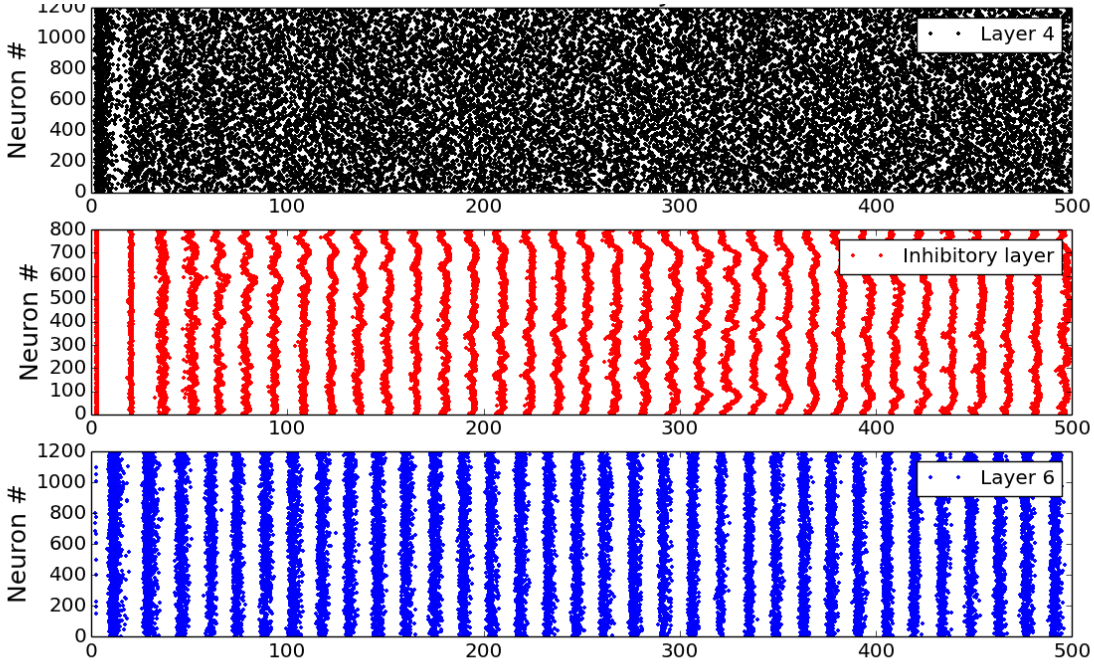

Figure 11: Small World Network with 0.025 mS gap junction conductance

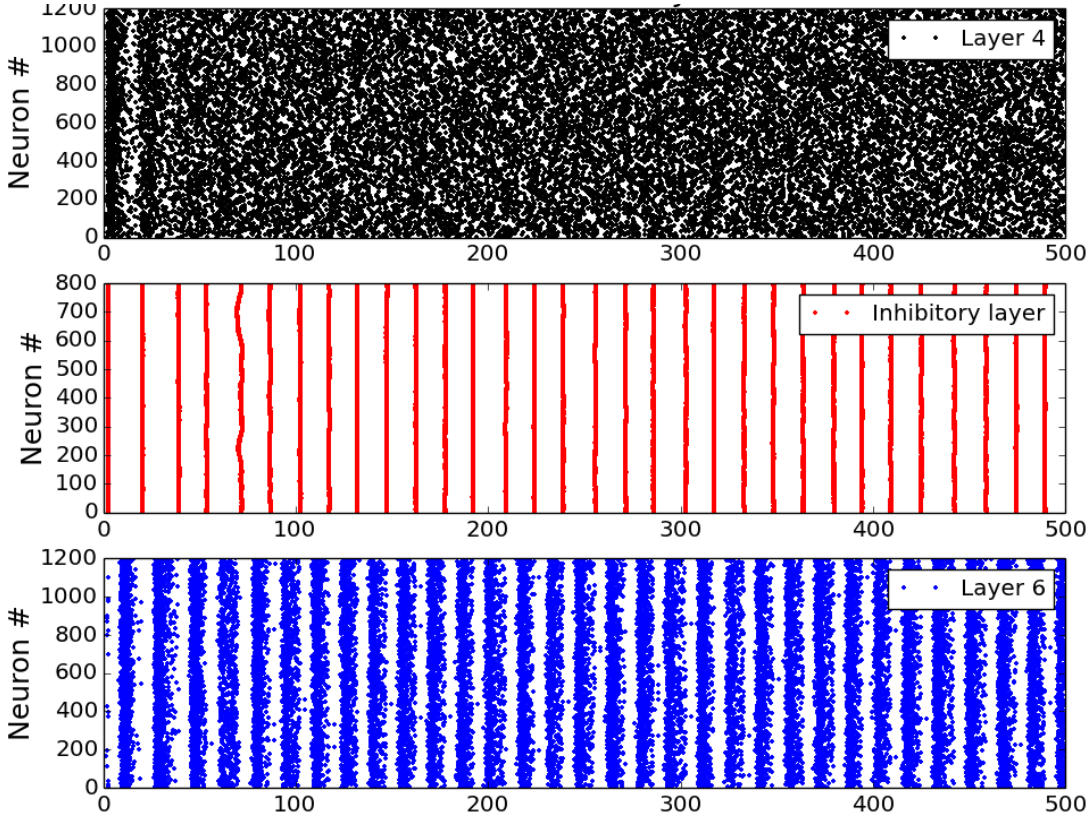

Figure 12: Small world network with 0.8 mS conductance

Acknowledgments

We would like to thank Professor Gert Cauwenberghs and Professor Gabriel Silva, as well Bruno Pedroni and Chul Kim for their help over the course of this class.

References

[1] Destexhe et al., Spatiotemporal analysis of LFP, J neuro 1999

[2] Maldonado P et al. Dynamics of striate cortical activity. Cereb Cortex 2000

[3] Shadlen MN, Newsome WT. Noise, neural codes and cortical organization. Curr Opin Neurobiol 4: 569–579, 1994.

[4] Softky WR, Koch C. The highly irregular firing of cortical cells is inconsistent with temporal integration of random EPSPs. J Neurosci 13: 334–350, 1993.

[5] Wang XJ. Neurophysiological and Computational Principles, Physiol. Rev.2010

[6] Newman MEJ. The structure and function of complex networks. *SIAM Review* 45(2), 167—256, 2003.

[7] Freeman WJ. Mass Action in the Nervous System. New York: Academic, 1975.

[8] Wang XJ, Buzsáki G. Gamma oscillation by synaptic inhibition in a hippocampal interneuronal network model. J Neurosci 16:6402–6413, 1996.

[9] Borhegyi Z, Varga V, Szilgyi N, Fabo D, Freund T. Phase segregation of medial septal GABAergic neurons during hippocampal theta activity. J Neurosci 24: 8470–8479, 2004.

[10] Shadlen MN, Newsome WT. Noise, neural codes and cortical organization. Current Opinions Neurobiology 4: 569–579, 1994.

[11] Wang XJ, Golomb D, Rinzel J. Emergent spindle oscillations and intermittent burst firing in a thalamic model: specific neuronal mechanisms. Proc Natl Acad Sci USA 92: 5577–5581, 1995.

[12] Andersen P, Eccles J. Inhibitory phasing of neuronal discharge. Nature 196: 645–647, 1962.